

The active site of *Tth*PolX is adapted to prevent 8-oxo-dGTP misincorporation

Patricia Garrido¹, Edison Mejia², Miguel Garcia-Diaz², Luis Blanco^{1,3} and Angel J. Picher^{1,*}

¹X-Pol Biotech S.L.U. Parque Científico de Madrid. Cantoblanco, Madrid 28049, Spain, ²Department of Pharmacological Sciences, Stony Brook University, Stony Brook, NY 11794, USA and ³Centro de Biología Molecular Severo Ochoa (CSIC-UAM). Cantoblanco, Madrid 28049, Spain

Received September 26, 2012; Revised September 4, 2013; Accepted September 5, 2013

ABSTRACT

Full genome sequencing of bacterial genomes has revealed the presence of numerous genes encoding family X DNA polymerases. These enzymes play a variety of biological roles and, accordingly, display often striking functional differences. Here we report that the PolX from the heat-stable organism *Thermus thermophilus* (*Tth*PolX) inserts the four dNTPs with strong asymmetry. We demonstrate that this behaviour is related to the presence of a single divergent residue in the active site of *Tth*PolX. Mutation of this residue (Ser²⁶⁶) to asparagine, the residue present in most PolXs, had a strong effect on *Tth*PolX polymerase activity, increasing and equilibrating the insertion efficiencies of the 4 dNTPs. Moreover, we show that this behaviour correlates with the ability of *Tth*PolX to insert 8-oxo-dGMP. Although the wild-type enzyme inefficiently incorporates 8-oxo-dGMP, the substitution of Ser²⁶⁶ to asparagine resulted in a dramatic increase in 8-oxo-dGMP incorporation opposite dA. These results suggest that the presence of a serine at position 266 in *Tth*PolX allows the enzyme to minimize the formation of dA:8-oxo-dGMP at the expense of decreasing the insertion rate of pyrimidines. We discuss the structural basis for these effects and the implications of this behaviour for the GO system (BER of 8-oxo-dG lesions).

INTRODUCTION

DNA polymerases are generally classified into seven families [the A, B, C, D, X, Y families and reverse transcriptases (1)]. Family X consists of specialized small DNA polymerases whose primary function is to fill gaps of one to a few nucleotides during DNA repair (2).

X-family DNA polymerases (PolXs) have moderate sequence conservation but are present in all kingdoms of life. In viruses, bacteria, archaea, protozoa and lower eukaryotes as well as in plants, only one PolX is present. However, vertebrates have four members (Polβ, Polλ, Polμ and TdT) that play different specific roles in a variety of processes such as DNA repair, V(D)J recombination and translesion synthesis (3,4).

Most PolX enzymes share a common modular organization (Polβ core) consisting of an 8-kDa domain and a 31-kDa polymerization domain comprising ‘fingers’, ‘palm’ and ‘thumb’ subdomains. This structural organization has been demonstrated for Polβ (5,6), TdT (7), Polλ (8,9), Polμ (10) and ASFV PolX (11,12).

DNA repair processes seek out DNA lesions, removing them from the DNA strands and repairing the genetic sequence at the site of the damaged bases. As an intermediate product of these DNA repair processes, single- and/or double-stranded gaps are created at certain points along the DNA. PolXs have evolved to accommodate these non-standard substrates and resolve the gaps. The unique structural feature that allows this family of enzymes to bind single- and/or double-strand gaps is the presence of an N-terminal 8-kDa domain upstream of the polymerization domain. The key role of this 8-kDa domain appears to be DNA binding, helping to position the enzyme on gapped or nicked substrates (5,6,13). For this purpose, the 8-kDa domain contains a Helix-hairpin-Helix motif that interacts with the DNA downstream to the gap in a non-sequence-dependent manner. Another mechanism through which the 8-kDa domain reinforces DNA binding is by interaction with the 5′-phosphate flanking the gap.

Oxidative DNA damage is caused by reactive oxygen species (ROS) generated in living cells during normal metabolism as well as by exogenous agents such as ionizing radiation and diverse chemical oxidants (14,15). Such ROS contribute to the rate of spontaneous mutation and have been implicated in aging and a number of diseases

*To whom correspondence should be addressed. Tel: +34 91 804 67 39; Fax: +34 91 806 30 90; Email: apicher@xpolbiotech.com

including cancer (16,17). The major oxidative base damage in DNA is the highly pre-mutagenic lesion 8-oxo-7,8-dihydro-2'-deoxyguanosine (8-oxo-dG) (18). Aside from guanine bases in the DNA, the dGTP pool is also targeted for oxidation, leading to formation of 8-oxo-dGTP (19). Either acting as a templating base or as an incoming nucleotide, the base 8-oxo-dG can correctly pair with dC, or incorrectly with dA (20), assuming the *syn* conformation and leading to Hoogsteen base pairing (21).

Complete sequencing of many bacterial genomes revealed the presence of genes encoding polymerases that belong to family X. Sequence analysis of bacterial PolXs indicated that they are structurally organized in two differentiated domains, the universal Pol β -like core and a C-terminal PHP (2). Unlike mammalian PolXs, the study of the cellular and molecular functions of bacterial PolXs has made little progress. A recent study revealed that PolX from the heat-stable organism *Thermus thermophilus* (*Tth*PolX) has DNA/RNA polymerase activity, as well as Mn²⁺-dependent exonuclease, 3'-phosphatase and apurinic/apyrimidinic endonuclease activities (22,23). Moreover, the crystal structures of *Tth*PolX in binary and ternary complexes have been recently reported, showing the structural basis of the kinetic mechanism of this enzyme, which binds Mg²⁺-dNTP before binding to DNA (24).

The present work describes the different ability of *Tth*PolX to insert each of the four possible dNTPs onto 1-nt gapped DNA molecules and the correlation of this behaviour with the ability of the polymerase to discriminate against 8-oxo-dGMP insertion. We discuss these results in the context of available crystal structures and discuss the implication of our findings considering the specific base-excision repair system for 8-oxo-dG operating in bacteria.

MATERIALS AND METHODS

Cloning of *Tth*PolX

Sequence analysis of the *T. thermophilus* HB8 genome (DDBJ/EMBL/GeneBank AB107660.1; GI:29603630) and *T. thermophilus* HB27 genome (DDBJ/EMBL/GeneBank AE017221.1; GI:46197919) revealed one ORF from each genome, TTHA1150 and TTC0785, respectively, encoding a protein that belongs to the PolX family. Using this sequence information, we synthesized two primers for amplification of the *Tth*PolX gene by PCR from *T. thermophilus* genomic DNA. The gene fragment amplified by PCR using Expand High Fidelity polymerase (Roche) was ligated into the pGEM T-easy vector (Promega) by TA cloning and confirmed by sequencing. Using the NdeI and EcoRI sites, the fragment bearing the target gene was ligated into pET28 vector (Novagen), which allows the expression of recombinant proteins as fusions with a multifunctional leader peptide containing a hexahistidyl sequence for purification on Ni²⁺-affinity resins. Site-directed mutations were introduced into *Tth*PolX expression plasmid by a PCR-based method (QuickChange Site-Directed Mutagenesis kit, Stratagene).

Overproduction and purification of *Tth*PolX

Expression of *Tth*PolX was carried out in the *Escherichia coli* strain BL21-CodonPlus (DE3)-RIL (Stratagene), with extra copies of the *argU*, *ileY* and *leuW* tRNA genes. Expression of *Tth*PolX was induced by the addition of 1 mM IPTG to 1.5 l of log phase *E. coli* cells grown at 30°C in LB to an Abs_{600nm} of 0.5. After induction, cells were incubated at 30°C for 5 h. Subsequently, the cultured cells were harvested, and the pelleted cells were weighted and frozen (−20°C). Just before purification, which was carried out at 4°C, frozen cells (5 g) were thawed and resuspended in 20 ml of buffer A [50 mM Tris-HCl (pH 7.5), 5% glycerol, 0.5 mM EDTA, 1 mM DTT] supplemented with 0.5 M NaCl and protease inhibitors and then disrupted by sonication on ice. Cell debris was discarded after a 5 min centrifugation at 3000 rpm. Insoluble material was pelleted by a 20 min centrifugation at 11 000 rpm. DNA was precipitated with 0.4% polyethyleneimine [10% stock solution in water (pH 7.5)] and sedimented by centrifugation for 20 min at 11 000 rpm. The supernatant was diluted to a final concentration of 0.25 M NaCl with buffer A and precipitated with ammonium sulphate to 50% saturation to obtain a polyethyleneimine-free protein pellet. This pellet was resuspended in buffer A without EDTA and 30 mM imidazole and loaded into a HisTrap HP column (5 ml, GE Healthcare) equilibrated previously in this buffer and 1 M NaCl. After exhaustive washing with buffer A and 1 M NaCl, proteins were eluted with a linear gradient of 30–250 mM imidazole. The eluate containing *Tth*PolX was diluted with buffer A to a final 0.1 M NaCl concentration and loaded into a monoS 4.6/100 PE column (1.7 ml, GE Healthcare), equilibrated previously in buffer A and 0.1 M NaCl. The column was washed, and the protein was eluted with a linear gradient of 0.1–0.5 M NaCl. Fractions containing *Tth*PolX were pooled, diluted to 0.2 M NaCl and loaded into a HiTrap Heparin HP column (5 ml, GE Healthcare), equilibrated previously in the same buffer. The column was washed, and the protein was eluted with a linear gradient of 0.2–0.5 M NaCl. Fractions containing *Tth*PolX were pooled, diluted again to 0.2 M NaCl and loaded into the same column, equilibrated previously in buffer A and 0.2 M NaCl. *Tth*PolX was eluted with buffer A with 1 M NaCl. This fraction contains highly purified (>99%) *Tth*PolX. Protein concentration was estimated by densitometry of Coomassie Blue-stained 10% SDS-polyacrylamide gels, using standards of known concentration. The final fraction, adjusted to 50% (v/v) glycerol, was stored at −70°C. The same protocol was used to purify the protein mutant S266N.

Kinetic analysis of DNA polymerization on 1-nt gapped molecules

Synthetic oligonucleotides purified by PAGE were obtained from Sigma. One nucleotide gapped molecules with a 5'-phosphate group were generated by annealing P1 primer (5' GATCACAGTGAGTAC) to four T13 templates (5' AGAAGTGTATCTXGTACTCACTGTGATC where X is A, C, G or T) and to downstream oligonucleotide Dg1P (5' AGATACACTTCT, with a 5' phosphate

group). P1 primer was fluorescently labelled at its 5'-end with Cy5. The primer was hybridized to template and downstream oligonucleotides to generate four different gapped molecules in the presence of 50 mM Tris-HCl (pH 7.5) and 0.3 M NaCl and heating to 80°C for 10 min before slowly cooling to room temperature over night. For single-turnover experiments, the incubation mixture contained, in 20 μ l, 50 mM Tris-HCl (pH 7.5), 10 mM MgCl₂, 1 mM DTT, 4% glycerol, 0.1 mg/ml bovine serum albumin, 5 nM of the DNA hybrid indicated in each case, 40 nM *Tth*PolX wild-type or mutant S266N and the indicated concentration of each dNTP. Reaction mixtures were incubated for 10 min at 37°C and stopped by adding 10 μ l of stop solution (10 mM EDTA and 97.5% deionized formamide). Steady-state analysis was performed in 20 μ l of reactions containing 50 mM Tris-HCl (pH 7.5), 1 mM DTT, 4% glycerol, 0.1 mg/ml bovine serum albumin, 10 mM MgCl₂, 200 nM DNA substrate and 4–40 nM protein. Reactions were initiated by mixing the nucleotide at different concentrations (2.5 μ M–10 pM, except for incorporation of 8-oxo-dGMP opposite C, where the concentrations used were 100–0.1 μ M) and incubated at 37°C for 12 min. Reactions were stopped by adding 10 μ l of stop solution. Extension of the labelled primer strand was analysed by 8 M urea and 20% PAGE and visualized using a Typhoon 9410 scanner (GE Healthcare). Gel band intensities were quantified using ImageQuant TL software (GE Healthcare). For single-turnover experiments, the observed rate of nucleotide incorporation (inferred from the amount of extended primer) was plotted as a function of nucleotide concentration. The values plotted are the mean of at least three independent experiments. For steady-state experiments, data were fit to the Michaelis-Menten equation using non-linear regression.

RESULTS

*Tth*PolX shows higher dNTP insertion efficiencies when the incoming dNTP is a purine

To characterize the DNA polymerization activity of *Tth*PolX, we tested different *in vitro* assay conditions using defined templated-DNA molecules. As previously reported by Nakane *et al.* (22), *Tth*PolX was able to catalyse dNTP incorporation efficiently in 1-nt gapped substrates in a dNTP dosage-dependent manner. As described for other PolX enzymes (13,25), we observed a significant increase in the polymerization activity when a phosphate group was present at the 5'-side of the gap compared with the same gapped DNA molecule having a hydroxyl group at its 5' end (Supplementary Figure S1). Therefore, in our assay conditions, *Tth*PolX shows a preference for small gaps with a 5'-phosphate group.

Accordingly, we then analysed the incorporation efficiency for each of the four possible dNTPs onto 1-nt gapped DNA molecules having a phosphate group at the 5' end of the gap by *Tth*PolX (Figure 1). When the incoming dNTP has a purine (dGTP or dATP), the reaction efficiency was higher than when the dNTP has a pyrimidine (dTTP or dCTP). This difference was

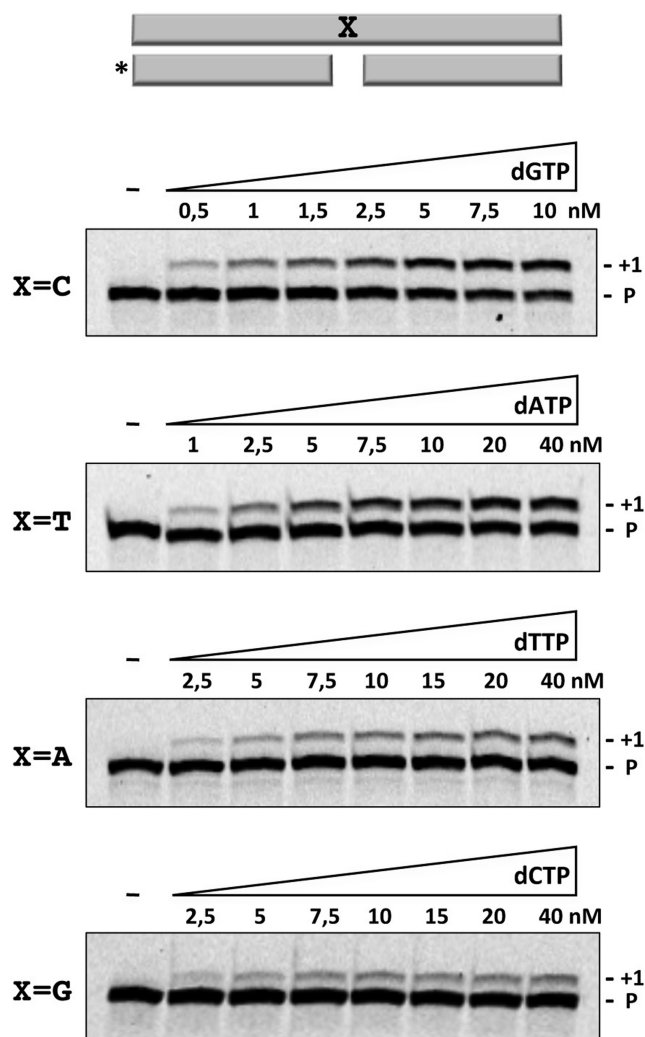


Figure 1. Gap-filling synthesis by *Tth*PolX. Incorporation rate of each complementary dNTP as a function of its concentration. Extension of the 5' end labelled primer (asterisk) was examined by PAGE. Reactions were carried out as described in 'Materials and Methods' section using the indicated concentrations of each dNTP.

investigated using the same defined DNA molecules and single turnover conditions, where the enzyme concentration is higher than the concentration of DNA (see 'Materials and Methods' section). Single turnover analysis of dNTP incorporation clearly revealed that *Tth*PolX showed a strong preference for purines. Quantification of the incorporation efficiency of each complementary dNTP demonstrated a strong imbalance, with a strong preference for purines: dG > dA > dT > dC (Supplementary Figure S2).

To obtain quantitative data and to confirm this conclusion, we performed several kinetic analysis under steady-state conditions. As shown in Table 1, the catalytic efficiency of dGTP incorporation by *Tth*PolX was 12-fold higher than dTTP. Thus, when the incoming nucleotide base is a pyrimidine, the incorporation efficiency appears to decrease dramatically (further discussed later).

Table 1. Steady-state kinetic parameters of insertion by *Tth*PolX and mutant S266N

Protein	Template	dNTP	k_{cat} (s^{-1})	K_m (nM)	Cat. eff. ($s^{-1} nM^{-1}$)
Wild-type	dC	dGTP	$(6.1 \pm 4) \times 10^{-3}$	4.9 ± 2.7	$(1.2 \pm 0.3) \times 10^{-3}$
	dA	dTTP	$(1.6 \pm 1) \times 10^{-3}$	13.4 ± 1.4	$(0.1 \pm 0.08) \times 10^{-3}$
	dC	8-oxo-dGTP	$(0.5 \pm 0.2) \times 10^{-3}$	3208 ± 1545	$(0.15 \pm 0.06) \times 10^{-6}$
	dA	8-oxo-dGTP	$(0.8 \pm 0.1) \times 10^{-3}$	126 ± 7	$(6.5 \pm 1) \times 10^{-6}$
S266N	dC	dGTP	$(14 \pm 1) \times 10^{-3}$	3.8 ± 0.9	$(4 \pm 1.6) \times 10^{-3}$
	dA	dTTP	$(7 \pm 3) \times 10^{-3}$	4.9 ± 0.3	$(1.5 \pm 0.7) \times 10^{-3}$
	dC	8-oxo-dGTP	$(0.6 \pm 0.2) \times 10^{-3}$	2396 ± 735	$(0.31 \pm 0.2) \times 10^{-6}$
	dA	8-oxo-dGTP	$(4.3 \pm 0.9) \times 10^{-3}$	37 ± 9	$(125 \pm 50) \times 10^{-6}$

Data are means (\pm standard error) of at least three independent experiments.

Ser²⁶⁶ of *Tth*PolX could be responsible for the low insertion efficiency of pyrimidine nucleotides

X-ray crystal structures of human Pol β indicate that Asn²⁷⁹ mediates one of the few interactions between the enzyme and the incoming nucleotide (26). More specifically, the ND2 amino group of the Asn²⁷⁹ side chain establishes a sequence independent hydrogen bond with the O2/N3 hydrogen bond acceptors in the minor groove of the incoming nucleotide. This would therefore imply a role of Asn²⁷⁹ in the formation of the correct base pair between the templating base and the incoming nucleotide. Interestingly, a multiple amino acid sequence alignment of the palm/thumb subdomain region of bacterial/archaeal family X DNA polymerases (Figure 2) revealed that this asparagine is highly conserved in PolX enzymes (bacteria: 80% of the cases in public databases; archaea: 94%). Strikingly, most members from the *Thermales* order have a serine substituting this asparagine (indicated with an arrow in Figure 2).

The conservation of the asparagine equivalent to human Pol β Asn²⁷⁹ from bacteria to humans supports an important role of this residue during catalysis. Conversely, the serine present at this position in *Tth*PolX would not be able to produce the same interactions with the nascent base pair, owing to its smaller side chain. This suggested that *Tth*PolX residue Ser²⁶⁶ could be responsible for the decrease in the catalytic efficiency when the incoming dNTP is a pyrimidine.

*Tth*PolX mutant S266N shows higher dNTP insertion efficiency than the wild-type enzyme

We hypothesized that Ser²⁶⁶ might be the residue responsible for the different insertion efficiency between purines and pyrimidines. To check this, we mutated Ser²⁶⁶ to asparagine, to restore the consensus of family X DNA polymerases.

Quantification of the incorporation efficiency of each complementary dNTP under single turnover conditions showed that the *Tth*PolX mutant S266N inserts the four dNTPs onto DNA with higher efficiency than the wild-type enzyme under linear and saturated conditions (Figure 3). Interestingly, the improvement was larger when the incoming dNTP was a pyrimidine, while purines just slightly increased their efficiencies.

To further confirm this observation, we performed the analysis under steady-state conditions. Steady-state

kinetic analysis demonstrated that the catalytic efficiency for dTTP incorporation by *Tth*PolX S266N was 15-fold higher than wild-type, whereas the increase observed in the case of dGTP incorporation was just 3-fold (Table 1).

In summary, we can conclude that the substitution of the original Ser²⁶⁶ of *Tth*PolX to the conserved residue (Asn) present in most family X polymerases produces an overall improvement in catalytic efficiency. However, the improvement is larger when the incoming nucleotide is a pyrimidine. As a result of this, the nucleotide insertion efficiency of mutant S266N is higher and more balanced between purines and pyrimidines than that of wild-type *Tth*PolX.

*Tth*PolX S266N retains the ability for faithful DNA synthesis

Previous studies reported a critical role of the human Pol β Asn²⁷⁹ residue in discriminating between the binding of correct and incorrect dNTPs (27). To analyse the capacity of *Tth*PolX mutant S266N to catalyse faithful DNA synthesis, each of the four dNTPs was assayed individually as a substrate to be incorporated opposite the four possible templating bases. In all cases, both wild-type *Tth*PolX and mutant S266N inserted the complementary dNTP, and not the incorrect three other nucleotides, even when provided at a 1000-fold higher concentration (Supplementary Figure S3).

Ser²⁶⁶ of *Tth*PolX protects against mutagenic incorporation of 8-oxo-dGTP

It was previously shown that mutation of Asn²⁷⁹ to alanine in human Pol β dramatically altered incorporation of 8-oxo-dGTP (28). Thus, whereas 8-oxo-dGTP was preferentially incorporated opposite a template dA versus dC (24:1) by wild-type hPol β , mutant N279A preferentially incorporated 8-oxo-dGTP opposite a template dC (1:14), mainly due to a dramatic decrease in the efficiency of incorporation opposite dA.

To study the possible impact of Ser²⁶⁶ of *Tth*PolX on 8-oxo-dGTP discrimination, we first compared, under single turnover conditions, the insertion opposite a template dC or a template dA by the wild-type *Tth*PolX versus mutant S266N (Figure 4). Wild-type *Tth*PolX preferentially incorporated 8-oxo-dGTP opposite dA rather than opposite dC. In both cases, the concentration of 8-oxo-dGTP required was much higher (>100-fold) than

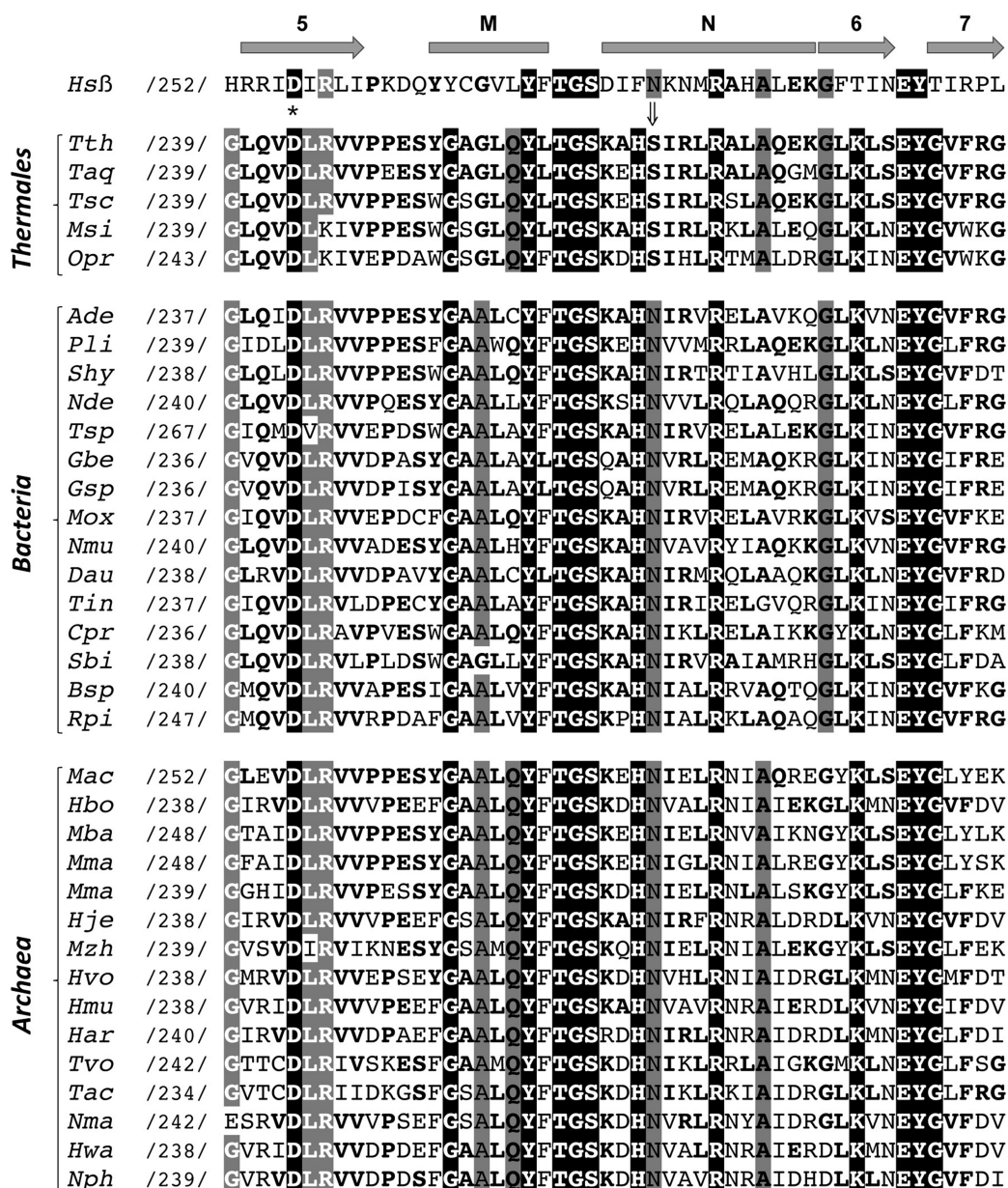


Figure 2. Multiple amino acid sequence alignment of the palm/thumb subdomain region of bacterial/archaeal family X DNA polymerases. *Tth*PolX amino acid sequence is the reference sequence in the alignment. By using *Tth*PolX sequence (residues 239–288) as a query against the database of nucleotide sequences previously translated in each of the six reading frames (www.ncbi.nlm.nih.gov/BLAST), we collected (shown here) the most similar PolXs present in species from bacteria and archaea kingdoms, regarding this particular amino acid segment. Numbers between slashes indicate the amino acid position relative to the N-terminus of each PolX. White bold letters boxed in black indicate invariant residues among PolXs. White bold letters boxed in grey indicate conserved residues in most PolXs. Black letters boxed in grey show residues that are invariant or highly conserved in at least two of the three groups (*Thermotales*, other bacteria or archaea) of PolXs aligned. An arrow indicates the only case in which an invariant residue (serine) in PolXs from *Thermotales* order is specifically different to another residue (an asparagine in this case), which is invariant in the rest of bacterial and archaeal PolXs. Human DNA polymerase β sequence and secondary elements (lettered α -helices and numbered β -strands) are also included in the alignment. An asterisk indicates one of the three catalytic aspartates. Names of organisms are abbreviated as follows (numbers in parentheses are GenBank accession numbers): *Tth*, *Thermus thermophilus* HB8 (BAD70973.1); *Taq*, *Thermus aquaticus* (BAA13425.1); *Tsc*, *Thermus scotoductus* (ADW21928.1); *Msi*, *Methanothermobacter thermoautotrophicus* (ADH63823.1); *Opr*, *Oceanithermus profundus* (ADR37134.1); *Ade*, *Ammonifex degensii* (ACX52880.1); *Pli*, *Planctomyces limnophilus* (ADG67560.1); *Shy*, *Streptomyces hygroscopicus* (AEY88391.1); *Nde*, *Nitrospira defluvii* (CBK43520.1); *Tsp*, *Thermodesulfobacterium* sp. (AEH23575.1); *Gbe*, *Geobacter bemidjiensis* (ACH37296.1); *Gsp*, *Geobacter* sp. (ACT16335.1); *Mox*, *Methylobacterium oxyfera* (CBE69823.1); *Nmu*, *Nitrosospora multififormis* (ABB74204.1); *Dau*, *Desulfuridus audaxviator* (ACA59665.1); *Tin*, *Thermodesulfatator indicus* (AEH44982.1); *Cpr*, *Coprothermobacter proteolyticus* (ACI17061.1); *Sbi*, *Streptomyces bingchengensis* (AD104058.1); *Bsp*, *Burkholderia* sp. (ADN60677.1); *Rpi*, *Ralstonia pickettii* (ACD29504.1); *Mac*, *Methanosarcina acetivorans* (AAM04167.1); *Hbo*, *Halogeometricum borinquense* (ADQ68029.1); *Mba*, *Methanosarcina barkeri* (AAZ70587.1); *Mma*, *Methanosarcina mazei* (AAM31590.1); *Mma*, *Methanohalophilus mahii* (ADE36598.1); *Hje*, *Halalkalicoccus jeotgali* (ADJ15891.1); *Mzh*, *Methanosalsum zhilinae* (AEH60552.1); *Hvo*, *Haloferax volcanii* (ADE03676.1); *Hmu*, *Halomicrobium mukohataei* (ACV49091.1); *Har*, *Halophilic archaeon* (AEN04653.1); *Tvo*, *Thermoplasma volcanium* (BAB60012.1); *Tac*, *Thermoplasma acidophilum* (CAC11891.1); *Nma*, *Natrialba magadii* (ADD04718.1); *Hwa*, *Haloquadratum walsbyi* (CCC39209.1); *Nph*, *Natronomonas pharaonis* (CA148518.1); *Hsβ*, *Homo sapiens* DNA polymerase beta (5423). Alignment was made by using the Multalin tool (<http://bioinfo.genopole-toulouse.prd.fr/multalin/multalin.html>).

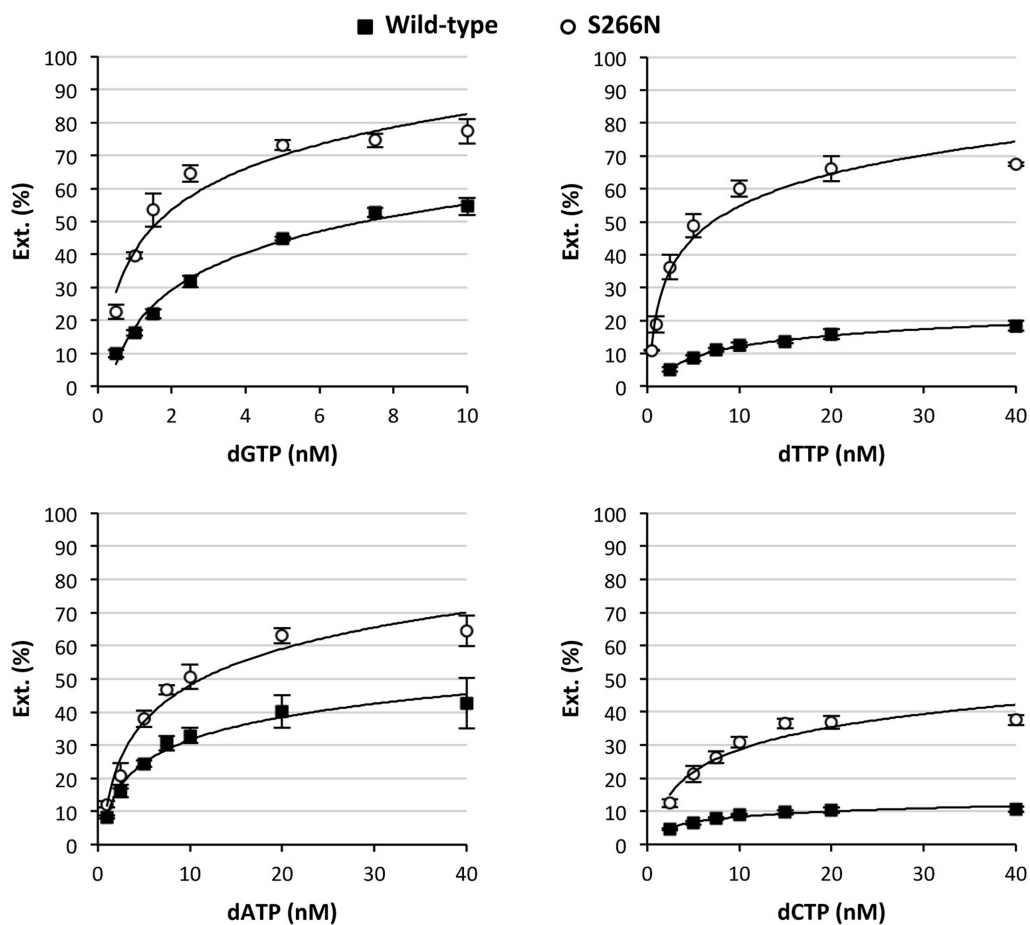


Figure 3. Mutation of Ser²⁶⁶ to asparagine increased dNTP insertion rate. Quantification of the complementary dNMP incorporation for the four 1-nt gapped molecules at different dNTP concentrations. The values plotted represent the ratio between the amounts of extended versus total primers and are the mean of at least three independent experiments.

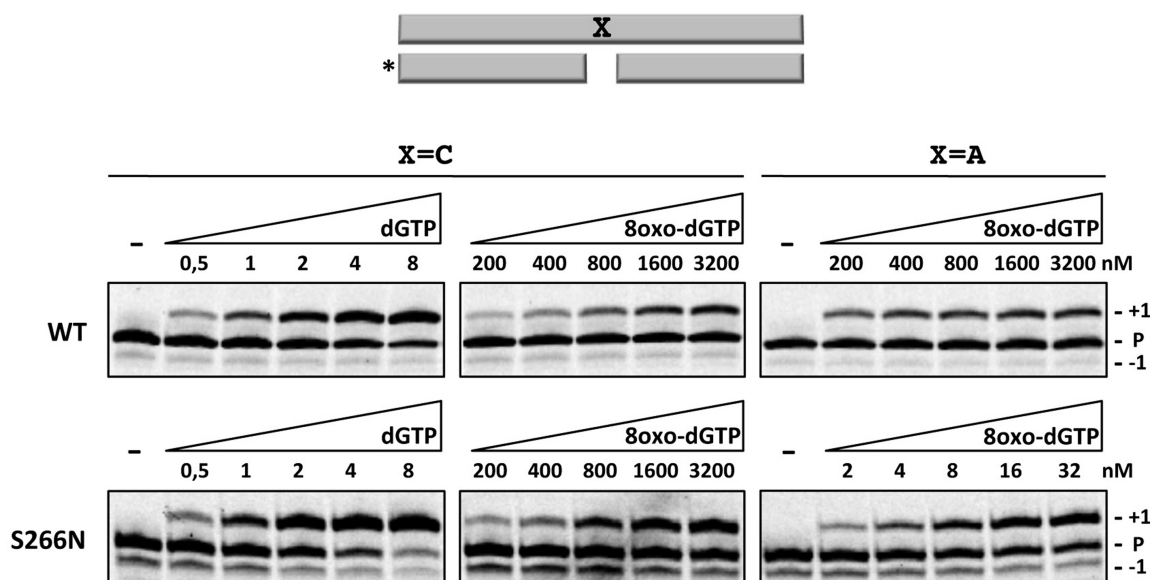


Figure 4. Mutation of Ser²⁶⁶ to asparagine specifically increased 8-oxo-dGMP insertion opposite a template dA by *Tth*PolX. Incorporation rate of each dNTP as a function of its concentration. Extension of the 5' end labelled primer (asterisk) was examined by PAGE. Reactions were carried out as described in 'Materials and Methods' section using the indicated concentrations of each dNTP.

the concentration of dGTP to be incorporated opposite a template dC. This indicates that *Tth*PolX has a strong discrimination against incorporation of 8-oxo-dGTP, regardless of the templating base (Figure 4, upper panels).

On the other hand, mutant S266N incorporated 8-oxo-dGTP opposite dC similarly to the wild-type (Figure 4, central panels), but required ~100-fold less 8-oxo-dGTP to reach wild-type levels of insertion opposite dA (Figure 4, right panels). Therefore, these qualitative results indicate that the *Tth*PolX S266N mutation largely improves the mutagenic incorporation of 8-oxo-dGTP opposite dA, being closer to the efficiency of incorporation of dGTP opposite dC than the wild-type *Tth*PolX.

Quantitative measurements under steady-state conditions showed that the incorporation efficiency of 8-oxo-dGTP opposite dC by *Tth*PolX S266N was about 2-fold better than wild-type (Table 1), similarly to the result with the undamaged dGTP. Remarkably, incorporation of 8-oxo-dGTP opposite dA by *Tth*PolX S266N was 19-fold more efficient than that by the wild-type *Tth*PolX (Table 1). As a result of this, insertion of 8-oxo-dGTP opposite dA by *Tth*PolX S266N is 403-fold more efficient than the insertion of 8-oxo-dGTP opposite dC, whereas for the wild-type this value is 43-fold (Table 1). This differential effect points to a crucial role of the serine residue at position 266 of *Tth*PolX in discriminating between alternative 8-oxo-dGTP conformations (*anti* for pairing with template dC and *syn* for Hoogsteen hydrogen bonding with template dA), being particularly relevant to avoid mutagenic incorporation of 8-oxo-dGTP.

DISCUSSION

Here we have shown that *Tth*PolX, a DNA polymerase likely involved in DNA repair, has an asymmetric use of dNTPs, favouring purines over pyrimidines. Moreover, our data showed that the oxidized nucleotide 8-oxo-dGTP is a poor substrate for incorporation by *Tth*PolX. Both features were related to the presence of a single serine residue (Ser²⁶⁶) instead of an asparagine that is highly conserved in most PolX enzymes. We have also shown that introducing that asparagine in *Tth*PolX equilibrates the efficiency of incorporation of the four dNTPs (favouring especially dTTP), but at the cost of an increase in the mutagenic insertion of 8-oxo-dGTP opposite dA.

The template base 8-oxo-dG has dual coding potential, due to its two possible conformations, either adopting an *anti* conformation to base-pair with incoming dCTP (error-free) or a *syn* conformation to base-pair with dATP (error-prone) through Hoogsteen hydrogen bonding. The oxidized nucleotide 8-oxo-dGTP has also dual base-pairing properties, although an intramolecular hydrogen bond between N2 of 8-oxo-dGTP and a non-bridging oxygen on the α -phosphate might strongly favour the *syn* conformation (29). Moreover, incorporation of 8-oxo-dGTP in the *anti* conformation seems to be unfavoured due to the steric repulsion between O8 and its sugar-phosphate backbone and also between O8 and the sugar (C2') of the primer 'terminus' (29). Consequently, most DNA polymerases prefer to insert 8-oxo-dGTP opposite a template dA.

Crystallographic structure analysis showed that during incorporation of 8-oxo-dGTP opposite dA by human Pol β , Asn²⁷⁹ forms a hydrogen bond with O8 of the incoming 8-oxo-dGTP in the *syn* conformation [Figure 5, part A; (29)], mimicking the minor groove hydrogen bond established by this residue with undamaged bases (26). Elimination of Asn²⁷⁹ in hPol β largely reduces the insertion of 8-oxo-dGTP opposite dA (28), confirming that Asn²⁷⁹ plays a stabilizing role that leads to the preferential formation of dA:8-oxo-dGMP versus dC:8-oxo-dGMP.

*Tth*PolX, as its closest orthologues from the *Thermales* order, have a serine (Ser²⁶⁶) in the equivalent position of hPol β Asn²⁷⁹ (Figure 2) likely unable to make the same contacts with the incoming 8-oxo-dGTP (modelled in

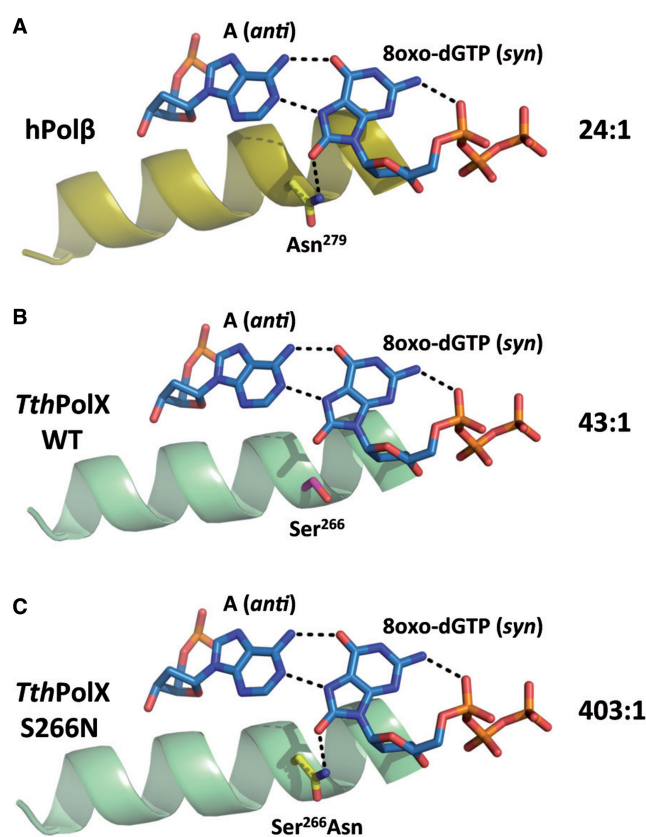


Figure 5. Structural basis for 8-oxo-dGMP incorporation by *Tth*PolX. Minor groove interactions with the incoming dNTP at the active sites of hPol β (PDB ID: 3MBY) and *Tth*PolX (PDB ID: 3AUO). (A) hPol β ternary complex. The *syn* conformation of the incoming 8-oxo-dGTP is stabilized through Hoogsteen hydrogen bonding with the templating adenine and a hydrogen bond with Asn²⁷⁹ of α -helix N. Additionally, an intra-molecular hydrogen bond between N2 of 8-oxo-dGTP and a non-bridging oxygen on the α -phosphate is shown. (B) The 3MBY model was overlaid on the *Tth*PolX structure (PDB ID: 3AUO; rmsd of 2.54 Å for 280 C- α atoms), and the nascent base pair is shown in (A) is rendered on the crystal structure of the *Tth*PolX ternary complex to evaluate the potential hydrogen bonding between Ser²⁶⁶ and 8-oxo-dGTP. The OG of Ser²⁶⁶ is 4.8 Å away from the O8 of 8-oxo-dGTP (C) The side chain of the Ser²⁶⁶ was replaced by the most common rotamer of asparagine in *Tth*PolX. The asparagine side chain seems to restore the capacity to form a hydrogen bond with the carbonyl group at C8 of the incoming 8-oxo-dGTP in the *syn* conformation. The ratios between incorporation efficiencies of 8-oxo-dGTP opposite dA and dC for each protein are shown on the right.

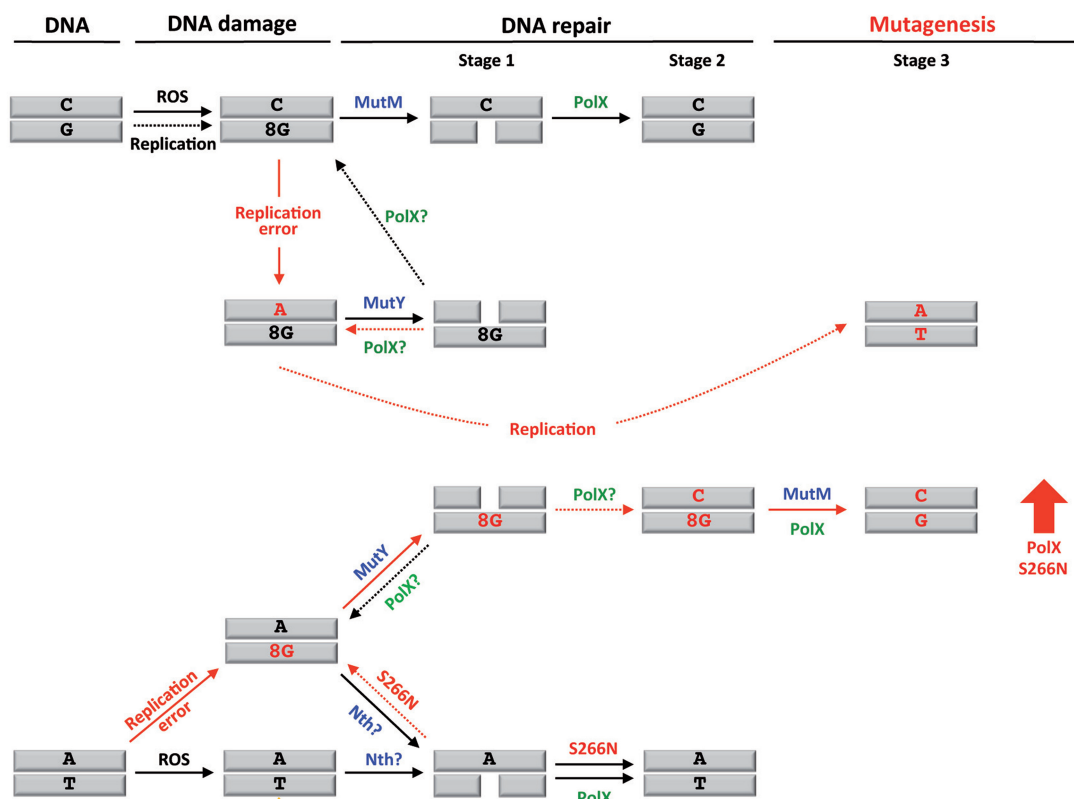


Figure 6. *Thermus thermophilus* GO system model. There are two possible pathways accumulating 8-oxo-dG onto DNA. (i) By ROS-mediated oxidation of a dC:dG base pair in DNA; (ii) During replication, and using the pool of 8-oxo-dGTP, 8-oxo-dGMP can be either inefficiently but correctly (opposite dC) incorporated or more efficiently inserted as an error (opposite dA). In the first two cases (upper part of the figure), MutM would recognize the dC:8-oxo-dG lesion and initiate the BER pathway, where *Tth*PolX would replace the correct (dG) nucleotide, as it is inefficient at inserting 8-oxo-dGMP opposite dC. If dC:8-oxo-dG remains unrepaired, a round of replication could incorporate an incorrect dAMP opposite 8-oxo-dG that, if further replicated, could trigger a CG→AT transversion. To minimize this, a second glycosylase (MutY) specifically eliminates the wrong nucleotide (dA), generating another chance to insert the correct nucleotide (dCMP) and thus regenerating the substrate for MutM-mediated BER. However, *Tth*PolX preferentially incorporate dAMP opposite 8-oxo-dG (data not shown), so either a different polymerase should be implicated in this step, or the presence of auxiliary proteins might favour the incorporation of dCMP opposite 8-oxo-dG by *Tth*PolX, as it has been recently demonstrated for human Polλ (34). Third, when 8-oxo-dGMP is frequently misincorporated opposite dA during replication (lower part of the figure), Nth glycosylase (35,36) could remove the damaged base. If not, MutY could gain access and remove dA (the correct base), and further BER events might lead to a transversion mutation (AT→CG). In this case, *Tth*PolX would promote the recovery of the original sequence, as it preferentially incorporates dAMP opposite 8-oxo-dG, generating another chance to initiate Nth-mediated BER and thus avoiding the transversion mutation AT→CG. In any case, either starting from a dA:8-oxo-dG mismatch or directly from a dA:dT-damaged base pair, Nth action would result in a gap that should be correctly filled in with the insertion of dTMP opposite template dA. As shown in this article, *Tth*PolX minimizes the insertion of 8-oxo-dGMP opposite dA during DNA repair, in part due to the Ser²⁶⁶ residue substituting the consensus Asn. Having such an Asn (as in mutant S266N) would lead to an increase in the incorporation of 8-oxo-dGMP opposite dA, promoting AT→CG transversion mutations. The BER proteins involved in each step are indicated (glycosylases in blue; wild-type *Tth*PolX in green; mutant S266N in red). Misincorporated nucleotides are highlighted in red. Red arrows indicate those processes and steps contributing to mutagenesis. Solid arrows indicate the most probable direction of the reaction for each substrate. Dashed arrows indicate other possible directions of the reaction for each substrate. The red arrow at the right indicates the possible increase in transversion mutagenesis (CG→AT) due to S266N mutation.

Figure 5, part B) and has also a preference to form dA:8-oxo-dGMP (Figure 4 and Table 1). Introduction of an asparagine instead of this serine (mutation S266N) produced an enormous increase in the efficiency of the mutagenic insertion of 8-oxo-dGTP opposite dA, whereas the 'correct' insertion opposite dC was not significantly improved (Figure 4 and Table 1). In summary, whereas the wild-type *Tth*PolX preferentially inserts 8-oxo-dGTP opposite dA versus dC, by a factor of 43-fold, mutant S266N inserts 8-oxo-dGTP opposite dA versus dC, by a factor of 403-fold. Thus, the lack of the Asn restricts the error-prone insertion of 8-oxo-dGTP opposite dA by ~10-fold.

As in hPolβ, the asparagine substitution of Ser²⁶⁶ could favour the formation of a hydrogen bond with O8 of the incoming 8-oxo-dGTP in the *syn* conformation (modelled in Figure 5, part C).

Introduction of the asparagine in *Tth*PolX also led to an overall improvement in nucleotide incorporation, more relevant for pyrimidines perhaps due to their smaller size and lesser important for the larger purines, as they would be sufficiently stabilized by stronger stacking interactions. A possible explanation for the stronger increase in dTMP incorporation could be that, when copying a dA template, the O2 of the incoming dTTP would be free to establish stabilizing hydrogen-bonding interactions with the

neighbour asparagine residue; conversely, when copying a dG, the O2 of the incoming dCTP would be already forming an hydrogen bond with the templating base, being less favoured by the stabilizing contribution of the asparagine.

The 'GO system', originally defined in *E.coli* (30), is a form of the base excision repair (BER) pathway to remove the lesion 8-oxo-dG. This system is conserved from bacteria to humans, and it comprises the MutM, MutY and MutT proteins (31). MutM is a glycosylase that removes 8-oxo-dG paired with dC. MutY is an adenine glycosylase that eliminates dA mispaired with 8-oxo-dG, when the favoured insertion of dAMP opposite 8-oxo-dG takes place during replication. Finally, MutT is a hydrolase that efficiently degrades 8-oxo-dGTP to 8-oxo-dGMP, reducing the availability of this oxidized dNTP for DNA polymerases. Heat-induced formation of ROS and 8-oxo-dG has been recently demonstrated (32). *Thermus thermophilus* is a thermophilic Gram-negative bacterium that grows aerobically at optimum temperatures ranging from 62 to 75°C, and, consequently, its MutT-based pathway to degrade 8-oxo-dGTP to 8-oxo-dGMP might not be able to sufficiently reduce the 8-oxo-dGTP concentration. This oxidized base would thus better compete with undamaged dNTPs for incorporation into DNA during replication and repair (Figure 6). Moreover, it is not yet clear which glycosylase would remove 8-oxo-dGMP misincorporated opposite dA, although it has been proposed that Nei and Nth could have also that role (33,35,36). However, Nei is not present in *T. thermophilus*. In such a context, preventing misincorporation of 8-oxo-dGTP, also during DNA repair, could be crucial to avoid mutagenesis in *T. thermophilus*. *TthPolX* might have adopted a structural solution to minimize the insertion of 8-oxo-dGTP opposite dA: by having Ser²⁶⁶ instead of the conserved asparagine at the nucleotide binding site, the efficiency of 8-oxo-dGTP incorporation is dramatically lower (by two magnitude orders).

In conclusion, *TthPolX* minimizes the risk of inserting 8-oxo-dGTP opposite dA by using a less efficient active site, and there are environmental and genetic reasons to explain the need for such an adaptation from a more general Pol β -like active site. However, it is tempting to speculate that *TthPolX* truly represents an ancestral version of this class of enzymes, originated to couple with higher loads of environmental damage. As soon as the GO system was perfected by evolution, and the environmental conditions were less prone to generating DNA damage, the PolX active site could also evolve, being upgraded by gaining an additional ligand (Asn) to favour a more balanced nucleotide incorporation efficiency.

SUPPLEMENTARY DATA

Supplementary Data are available at NAR Online.

ACKNOWLEDGEMENTS

The authors thank Drs S. H. Wilson and K. Bebenek for helpful discussions.

FUNDING

Spanish Ministry of Science and Innovation [CIT-010000-2008-6 and IPT-010000-2010-015 to A.J.P., BFU2009-10085 and CDS2007-0015 to L.B.]; Autonomous Community of Madrid [PIE/112/2010 to A.J.P.]; National Institutes of Health [R01 GM100021 to M.G.-D.]. Funding for open access charge: Spanish Ministry of Science and Innovation [IPT-010000-2010-015].

Conflict of interest statement. None declared.

REFERENCES

- Rothwell, P.J. and Waksman, G. (2005) Structure and mechanism of DNA polymerases. *Adv. Protein Chem.*, **71**, 401–440.
- Ramadan, K., Shevelev, I. and Hübscher, U. (2004) The DNA-polymerase-X family: controllers of DNA quality? *Nat. Rev. Mol. Cell Biol.*, **5**, 1038–1043.
- Hübscher, U., Maga, G. and Spadari, S. (2002) Eukaryotic DNA polymerases. *Annu. Rev. Biochem.*, **71**, 133–163.
- Yamitch, J. and Sweasy, J.B. (2010) DNA polymerase family X: function, structure, and cellular roles. *Biochim. Biophys. Acta.*, **1804**, 1136–1150.
- Pelletier, H., Sawaya, M.R., Kumar, A., Wilson, S.H. and Kraut, J. (1994) Structures of ternary complexes of rat DNA polymerase beta, a DNA template-primer, and ddCTP. *Science*, **264**, 1891–1903.
- Sawaya, M.R., Pelletier, H., Kumar, A., Wilson, S.H. and Kraut, J. (1994) Crystal structure of rat DNA polymerase beta: evidence for a common polymerase mechanism. *Science*, **264**, 1930–1935.
- Delarue, M., Boulé, J.B., Lescar, J., Expert-Bezançon, N., Jourdan, N., Sukumar, N., Rougeon, F. and Papanicolaou, C. (2002) Crystal structures of a template-independent DNA polymerase: murine terminal deoxynucleotidyltransferase. *EMBO J.*, **21**, 427–439.
- Garcia-Diaz, M., Bebenek, K., Krahn, J.M., Blanco, L., Kunkel, T.A. and Pedersen, L.C. (2004) A structural solution for the DNA polymerase lambda-dependent repair of DNA gaps with minimal homology. *Mol. Cell*, **13**, 561–572.
- Garcia-Diaz, M., Bebenek, K., Krahn, J.M., Kunkel, T.A. and Pedersen, L.C. (2005) A closed conformation for the Pol lambda catalytic cycle. *Nat. Struct. Mol. Biol.*, **12**, 97–98.
- Moon, A.F., Garcia-Diaz, M., Bebenek, K., Davis, B.J., Zhong, X., Ramsden, D.A., Kunkel, T.A. and Pedersen, L.C. (2007) Structural insight into the substrate specificity of DNA Polymerase mu. *Nat. Struct. Mol. Biol.*, **14**, 45–53.
- Maciejewski, M.W., Shin, R., Pan, B., Marintchev, A., Denninger, A., Mullen, M.A., Chen, K., Gryk, M.R. and Mullen, G.P. (2001) Solution structure of a viral DNA repair polymerase. *Nat. Struct. Biol.*, **8**, 936–941.
- Showalter, A.K., Byeon, I.J., Su, M.I. and Tsai, M.D. (2001) Solution structure of a viral DNA polymerase X and evidence for a mutagenic function. *Nat. Struct. Biol.*, **8**, 942–946.
- Prasad, R., Beard, W.A. and Wilson, S.H. (1994) Studies of gapped DNA substrate binding by mammalian DNA polymerase beta. Dependence on 5'-phosphate group. *J. Biol. Chem.*, **269**, 18096–18101.
- Breimer, L.H. (1990) Molecular mechanisms of oxygen radical carcinogenesis and mutagenesis: the role of DNA base damage. *Mol. Carcinog.*, **3**, 188–197.
- Ames, B.N. and Gold, L.S. (1991) Endogenous mutagens and the causes of aging and cancer. *Mutat. Res.*, **250**, 3–16.
- Epe, B. (1991) Genotoxicity of singlet oxygen. *Chem. Biol. Interact.*, **80**, 239–260.
- Fiala, E.S., Nie, G., Sodum, R., Conaway, C.C. and Sohn, O.S. (1993) 2-Nitropropane-induced liver DNA and RNA base modifications: differences between Sprague-Dawley rats and New Zealand white rabbits. *Cancer Lett.*, **74**, 9–14.
- Grollman, A.P. and Moriya, M. (1993) Mutagenesis by 8-oxoguanine: an enemy within. *Trends Genet.*, **9**, 246–249.

19. Fraga, C.G., Shigenaga, M.K., Park, J.W., Degan, P. and Ames, B.N. (1990) Oxidative damage to DNA during aging: 8-hydroxy-2'-deoxyguanosine in rat organ DNA and urine. *Proc. Natl Acad. Sci. USA*, **87**, 4533–4537.
20. Maki, H. and Sekiguchi, M. (1992) MutT protein specifically hydrolyses a potent mutagenic substrate for DNA synthesis. *Nature*, **355**, 273–275.
21. Krahn, J.M., Beard, W.A., Miller, H., Grollman, A.P. and Wilson, S.H. (2003) Structure of DNA polymerase beta with the mutagenic DNA lesion 8-oxodeoxyguanine reveals structural insights into its coding potential. *Structure*, **11**, 121–127.
22. Nakane, S., Nakagawa, N., Kuramitsu, S. and Masui, R. (2009) Characterization of DNA polymerase X from *Thermus thermophilus* HB8 reveals the POLXc and PHP domains are both required for 3'-5' exonuclease activity. *Nucleic Acids Res.*, **37**, 2037–2052.
23. Nakane, S., Nakagawa, N., Kuramitsu, S. and Masui, R. (2012) The role of the PHP domain associated with DNA polymerase X from *Thermus thermophilus* HB8 in base excision repair. *DNA Repair*, **11**, 906–914.
24. Nakane, S., Ishikawa, H., Nakagawa, N., Kuramitsu, S. and Masui, R. (2012) The structural basis of the kinetic mechanism of a gap-filling X-family DNA polymerase that binds Mg(2+)-dNTP before binding to DNA. *J. Mol. Biol.*, **417**, 179–196.
25. Garcia-Diaz, M., Bebenek, K., Sabariego, R., Dominguez, O., Rodriguez, J., Kirchhoff, T., Garcia-Palomero, E., Picher, A.J., Juarez, R., Ruiz, J.F. *et al.* (2002) DNA polymerase lambda, a novel DNA repair enzyme in human cells. *J. Biol. Chem.*, **277**, 13184–13191.
26. Sawaya, M.R., Prasad, R., Wilson, S.H., Kraut, J. and Pelletier, H. (1997) Crystal structures of human DNA polymerase beta complexed with gapped and nicked DNA: evidence for an induced fit mechanism. *Biochemistry*, **36**, 11205–11215.
27. Kraynov, V.S., Werneburg, B.G., Zhong, X., Lee, H., Ahn, J. and Tsai, M.D. (1997) DNA polymerase beta: analysis of the contributions of tyrosine-271 and asparagine-279 to substrate specificity and fidelity of DNA replication by pre-steady-state kinetics. *Biochem. J.*, **323**, 103–111.
28. Miller, H., Prasad, R., Wilson, S.H., Johnson, F. and Grollman, A.P. (2000) 8-oxodGTP incorporation by DNA polymerase beta is modified by active-site residue Asn279. *Biochemistry*, **39**, 1029–1033.
29. Batra, V.K., Beard, W.A., Hou, E.W., Pedersen, L.C., Prasad, R. and Wilson, S.H. (2010) Mutagenic conformation of 8-oxo-7,8-dihydro-2'-dGTP in the confines of a DNA polymerase active site. *Nat. Struct. Mol. Biol.*, **17**, 889–890.
30. Michaels, M.L. and Miller, J.H. (1992) The GO system protects organisms from the mutagenic effect of the spontaneous lesion 8-hydroxyguanine (7,8-dihydro-8-oxoguanine). *J. Bacteriol.*, **174**, 6321–6325.
31. Slupphaug, G., Kavli, B. and Krokan, H.E. (2003) The interacting pathways for prevention and repair of oxidative DNA damage. *Mutat. Res.*, **531**, 231–251.
32. Bruskov, V.I., Malakhova, L.V., Masalimov, Z.K. and Chernikov, A.V. (2002) Heat-induced formation of reactive oxygen species and 8-oxoguanine, a biomarker of damage to DNA. *Nucleic Acids Res.*, **30**, 1354–1363.
33. Hazra, T.K., Izumi, T., Venkataraman, R., Kow, Y.W., Dizdaroglu, M. and Mitra, S. (2000) Characterization of a novel 8-oxoguanine-DNA glycosylase activity in *Escherichia coli* and identification of the enzyme as endonuclease VIII. *J. Biol. Chem.*, **275**, 27762–27767.
34. Maga, G., Villani, G., Crespan, E., Wimmer, U., Ferrari, E., Bertocci, B. and Hübscher, U. (2007) 8-oxo-guanine bypass by human DNA polymerases in the presence of auxiliary proteins. *Nature*, **447**, 606–608.
35. Matsumoto, Y., Zhang, Q.M., Takao, M., Yasui, A. and Yonei, S. (2001) *Escherichia coli* Nth and human hNTH1 DNA glycosylases are involved in removal of 8-oxoguanine from 8-oxoguanine/guanine mispairs in DNA. *Nucleic Acids Res.*, **29**, 1975–1981.
36. Suzuki, T., Yamamoto, K., Harashima, H. and Kamiya, H. (2008) Base excision repair enzyme endonuclease III suppresses mutagenesis caused by 8-hydroxy-dGTP. *DNA Repair*, **7**, 88–94.